

SHOCK DAMPING IN A Cu-Zn-Al SHAPE MEMORY ALLOY

J.MULLER (a), B.DUBOIS (b), J.CONDOURE (c), J.F.FRIES (c)

(a) Centre de Recherches de Voreppe, CRV SA, BP 27, 38340 VOREPPE, FRANCE

(b) Laboratoire de Métallurgie Appliquée, ENSCP, 11 rue Pierre et Marie Curie, 75231 PARIS Cedex 05, FRANCE

(c) Centre de Recherches des Matériaux, GIAT INDUSTRIES Centre de Tarbes, BP 1450, 65014 TARBES Cedex, FRANCE

ABSTRACT

In order to precise high damping capacity of shape memory alloys (SMA), an extension from internal friction to shock damping capacity is proposed. For any metallic material submitted to a limited plastic deformation at high strain rates (from 10^{-3} to 5000 s^{-1}), a damping power concept Q^{-1} is introduced and related to some aspects of the mechanical energy dissipation. Experiments were performed with a quadrant shock pendulum and Hopkinson split bars. In a Cu-27,6wt% Zn - 3,63wt% Al- 0,6wt% B SMA, adiabatic shear bands and shock induced martensites are observed. This would be an accommodation process for shock damping.

1. INTRODUCTION

Damping in shape memory alloys seems to be a worthwhile topic since they give an anormal ringing noise when beaten in the as quenched martensitic state. Under cyclic sollicitations, at quite low frequencies, internal friction Q^{-1} is related to the stress-strain curve (fig. 1). However, even at high frequencies, the stress is too low to compare to practical applications.

The thermomechanical martensite transformation is found responsible for the high internal friction [1 to 8]. All these descriptions are valuable for quasi-static sollicitations and we would like to know the loss energy of SMA alloy in dynamic sollicitation like shock damping, crash,...as OGAWA [9] has already mentioned.

The present paper is an essay to describe an unique unified approach of mechanical damping, its characterization and some observations related to the Cu-Zn-Al SMA alloy.

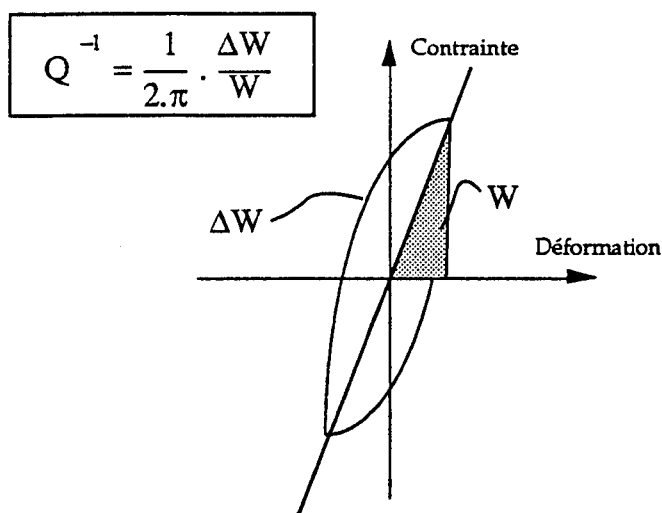


Figure 1 : Internal damping measurement

2. UNIFIED DEFINITION OF MECHANICAL DAMPING CAPACITY

In order to find the influence of the microstructural evolutions during dynamic loadings on what we could call the loss energy capacity, a parameter call "damping power" Ω^{-1} is suggested (fig. 2). It is obtained from the stress-strain curve after a mechanical test either in static or dynamic conditions. By comparison with internal friction, we shall write

$$\Omega^{-1} = \frac{\Delta W_{\text{total}}}{W_{\text{total}}}$$

where

$$\Delta W_{\text{total}} = \int_0^{\varepsilon_{\text{max}}} \sigma \cdot d\varepsilon - \frac{\sigma^2}{2E}$$

(E is the Young modulus)

$$\text{and } W_{\text{total}} = \frac{1}{2} \cdot E \cdot \varepsilon_{\text{max}}^2$$

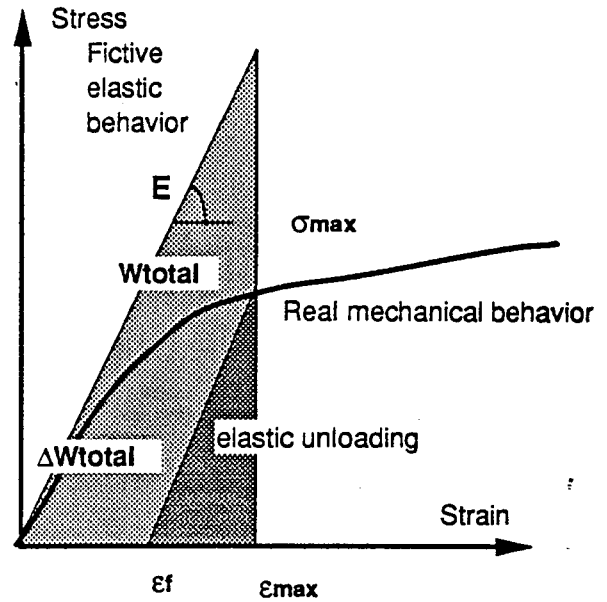


Figure 2 : Unified approach to mechanical damping capacity

The "damping power" Ω^{-1} depends on the strain rate $\dot{\varepsilon}$, since the volume fraction of the sample sollicitated by the dynamic stress is supposed to be a function of the strain rate [10]. In this conditions, the dynamic stress could be written by the equation :

$$\sigma(\varepsilon, \dot{\varepsilon}) = \sigma(\varepsilon, \dot{\varepsilon}_0) + \beta \cdot \log\left(\frac{\dot{\varepsilon}}{\dot{\varepsilon}_0}\right)$$

The variations of the β parameter with the strain rate, not given in this work, confirm the dependence of Ω^{-1} with dynamic sollicitation.

$\sigma_{st}(\varepsilon, \dot{\varepsilon}_0)$	<i>quasi static stress at deformation ε with a strain rate of 10^{-3} s^{-1}</i>
$\sigma(\varepsilon, \dot{\varepsilon})$	<i>Dynamic stress at deformation ε and strain rate $\dot{\varepsilon}$</i>
β	<i>is the strain rate sensitivity</i>

3. EXPERIMENTAL METHODS

Cylindrical specimens (8 mm of length and diameter) were machined from a Cu-27.6wt% Zn - 3.63wt% Al- 0.6wt% B shape memory alloy (TREFIMETAUX Company). The samples were heat treated at 1123 K for 15 mn, before water quenching at 273 K.

Phase transformation temperatures were characterized both by electrical resistivity measurements and differential calorimetry (on a METTLER DSC 30). Results are in table 1. X-ray diffraction analysis showed that specimens contained about 15% of martensite phases (9R and 18R) at room temperature.

	Differential calorimetry	Electrical resistivity
Ms	232 K	227 K
Mf	182 K	193 K
As	238 K	215 K
Af	258 K	243 K

Static compression test were carried out at 10^{-3} s^{-1} on an INSTRON machine. Dynamic compression loadings were obtained on a quadrant shock pendulum until 700 s^{-1} (GIAT INDUSTRIES, fig.3), and split Hopkinson bars from $9 \cdot 10^2$ to $3 \cdot 10^3 \text{ s}^{-1}$ (Ecole Centrale de Nantes, fig.5). Experimental raw datas are presented on figures 4,5,6 before stress-strain conversion. A thermocouple was attached to some specimens and the temperature was monitored during and after the test, for measuring the temperature increase from the plastic energy degradation. After tests, shocked samples were examined by optical microscopy. The transformation temperatures were measured again by DSC. X-ray diffraction analysis was used to control phases and to measure the whole volume fraction of transformed product.

Table 1 : Phase transformation temperature of initial state

Static compression test were carried out at 10^{-3} s^{-1} on an INSTRON machine. Dynamic compression loadings were obtained on a quadrant shock pendulum until 700 s^{-1} (GIAT INDUSTRIES, fig.3), and split Hopkinson bars from $9 \cdot 10^2$ to $3 \cdot 10^3 \text{ s}^{-1}$ (Ecole Centrale de Nantes, fig.5). Experimental raw datas are presented on figures 4,5,6 before stress-strain conversion. A thermocouple was attached to some specimens and the temperature was monitored during and after the test, for measuring the temperature increase from the plastic energy degradation. After tests, shocked samples were examined by optical microscopy. The transformation temperatures were measured again by DSC. X-ray diffraction analysis was used to control phases and to measure the whole volume fraction of transformed product.

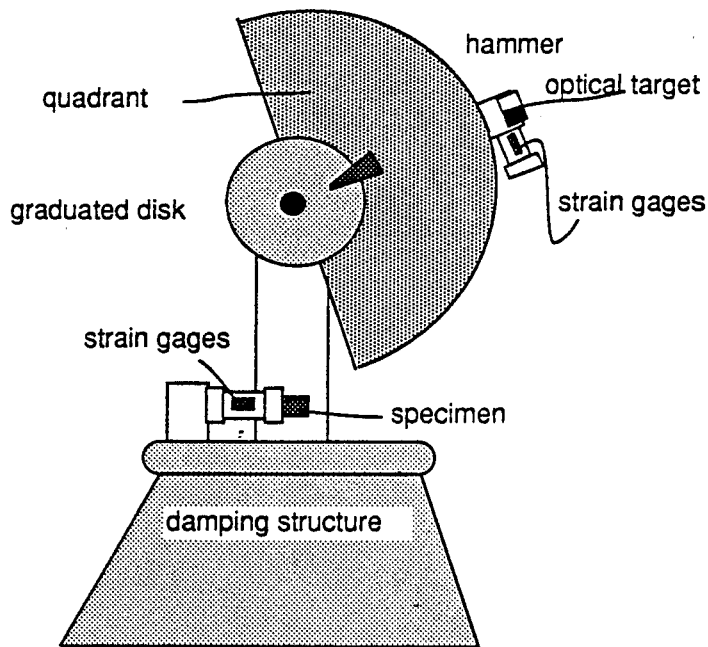


Figure 3 : Quadrant shock pendulum allows to explore strain rates between 200 and 800 s⁻¹. Energy of shocks is between 15 and 60 J during 2 ms.

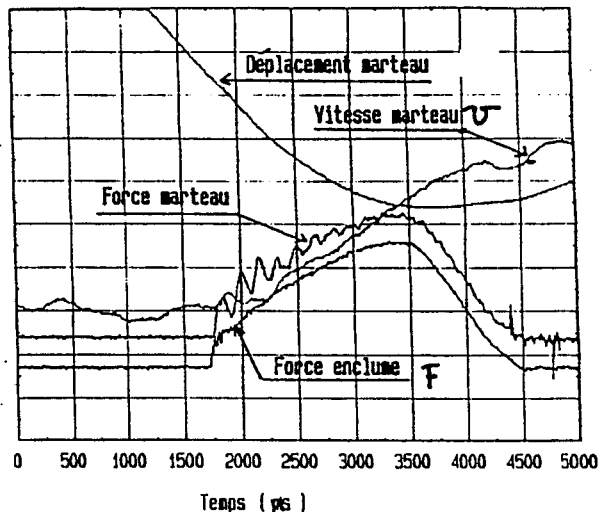


Figure 4 : Typical experimental load, displacement and speed curve vs time for one shock with quadrant pendulum

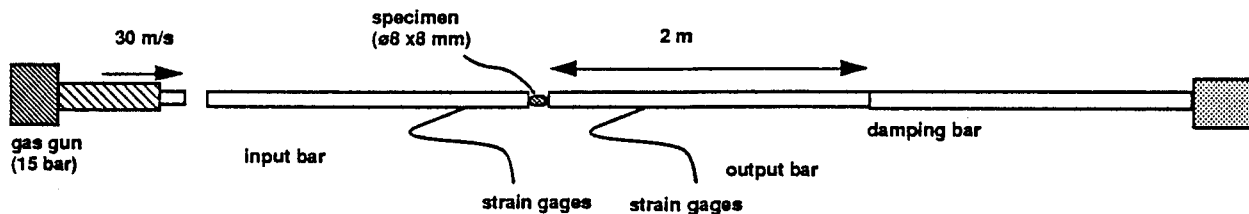


Figure 5 : Split Hopkinson bar apparatus allows high strain rates until 3000 s⁻¹. Energy of shocks is around 300 J during 200 µs.

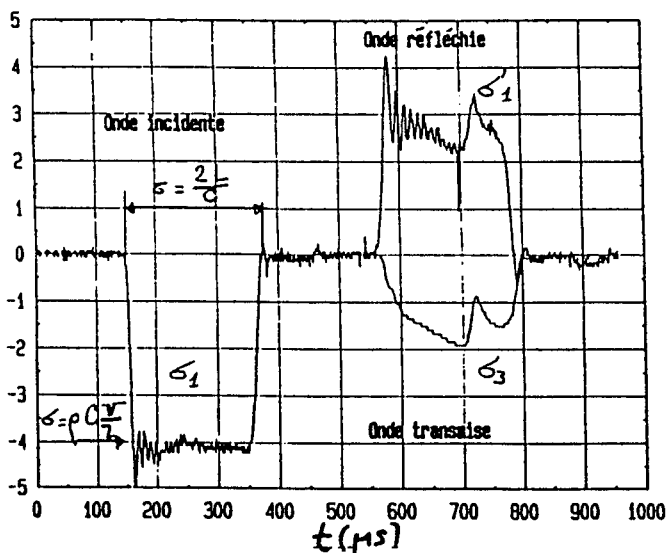


Figure 6 : (split Hopkinson bars) Typical experimental recording from strain gages. Incident wave is separated into a transmitted one and a reflected one.

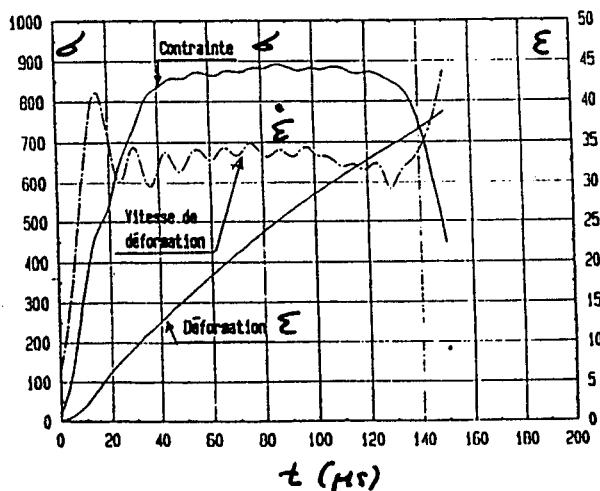


Figure 7 : (idem) From the curves of fig.6, calculation give the mean stress, strain and strain rate vs time.

4. EXPERIMENTAL RESULTS

4.1. Strain, strain evolutions from static to dynamic loadings.

Stress-strain curves are plotted on fig.9 for some typical strain rates obtained with the two experimental apparatus. A quasi continuous evolution is observed from static curves to those obtained at mean and high strain rates. The Cu-Zn-Al SMA studied is very sensible to the strain rate, particularly in the 3-5% deformation domain. The observed evolution is shown for several tests (at least three tests by strain rate). The variations of the corresponding "damping power" Ω^{-1} versus strain rate are presented on fig.10.

At very high strain rates, there is some doubt about the datas because all the physical hypothesis are not satisfied for stress-strain calculations. When strain rate is near 2000 s^{-1} , the uniaxial stress way can change to an uniaxial deformation way. Finally only mean and high strain rates increase the dynamic damping of the studied alloy. The results are in agreement with those obtained on Cu-Al-Ni and Fe-Mn-si SMA [10]. Furthermore it was noticed that in classical metals and alloys, the temperature increase during the shock is higher than in SMA.

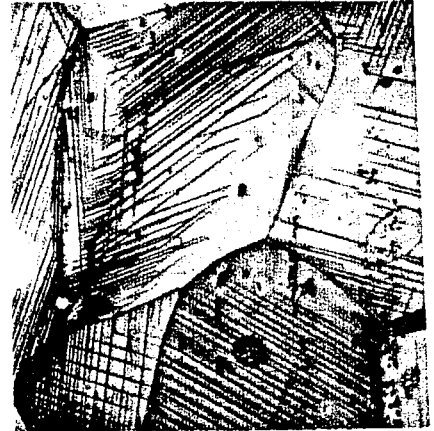


Figure 8: Initial quasi austenitic microstructure before testing

4.2. Optical microscopy

The shocked specimens presented many different inhomogeneous aspects. It was difficult to relate clearly an evolution of microstructure to the shock energy or the shock strain rate. However in several specimens, the heterogeneous structures showed a very strong localization of deformation that we thought of adiabatic shear bands. Finally an interpretation was built by ranging our observations in two classes. It appeared that the shocked microstructures were the

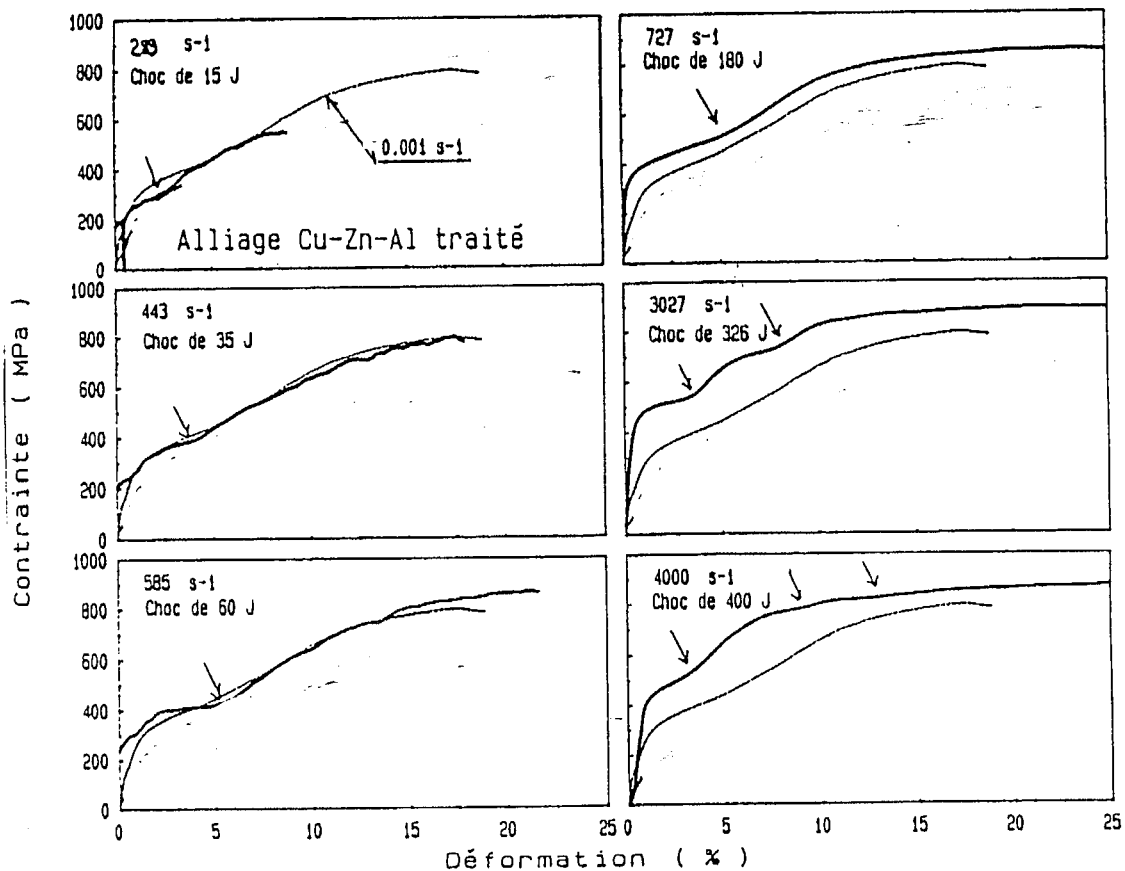


Figure 9 : Influence of strain rate on experimental stress-strain curves. Each test (solid line) is compared to the static test (light line).

result either of changes of the initial structures by phase transformation, or a consequence of the stress waves generated by the uniaxial compression of our samples.

In the first group, three morphologies of martensite products were distinguished (fig. 11,12,13). The result is supported by X-ray diffraction : it was thought of 6R and 2H martensite, according to the macroscopic scale of observation. Furthermore the volume fraction of martensite decreases from the impact to the limit of the sample (from 80% to 30%). It is recalled that only 15% was found in the initial state.

The second group would be called "generated defects" (fig.14,15,16). It seems that the initial structure was completely changed in a cold or hot worked damaged structures. Cracks and cavities were detected, sometimes in the adiabatic shear bands. It would be the result of a high plastic deformation rather than other physical transformation. We did not

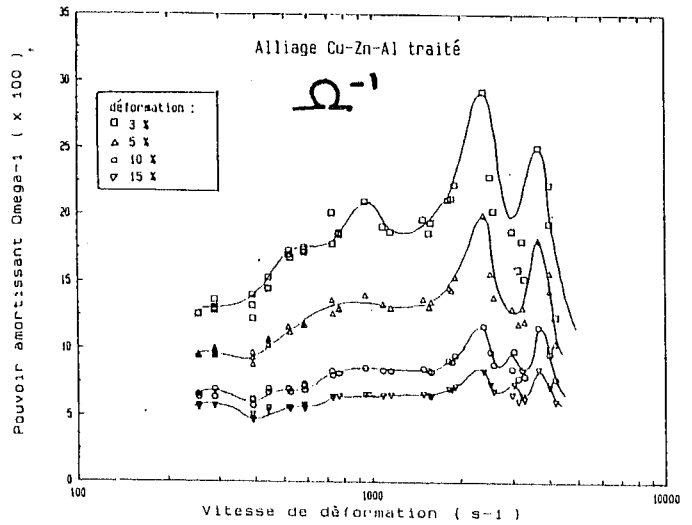


Figure 10 : Evolution of the "damping power" Ω^{-1} with strain rate from mean to high strain rates. Some reserves have to be made for strain rates $> 2000 \text{ s}^{-1}$.



Figure 11 : Transformation product generated by impact

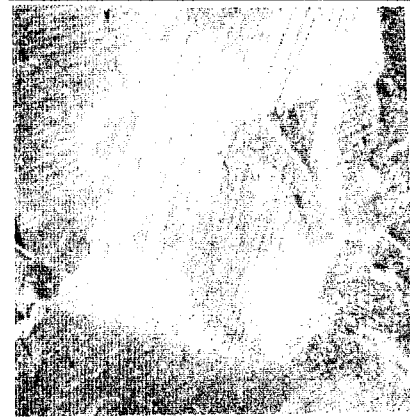


Figure 12 : Transformation product of pre-existing martensite, modified during the test.

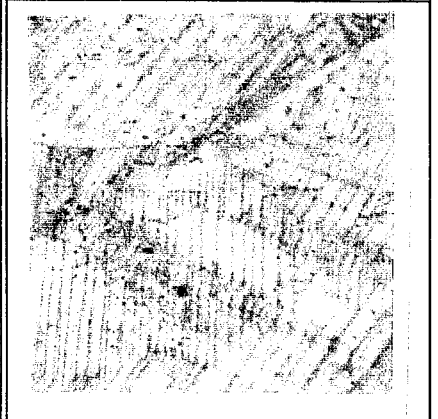


Figure 13 : Transformation product, which have been plastically deformed during the test

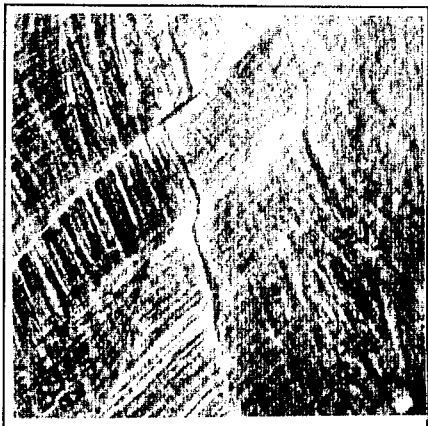


Figure 14: Shear plastic instabilities (mainly adiabatic).

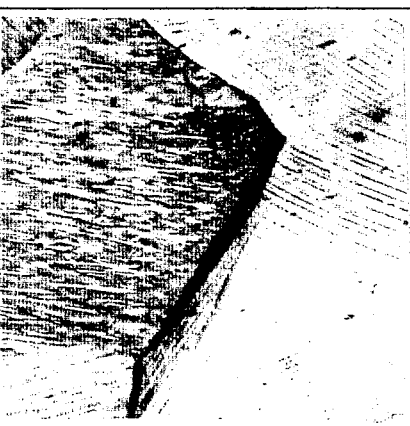


Figure 15 : Intergranular cracking (grains decohesion)

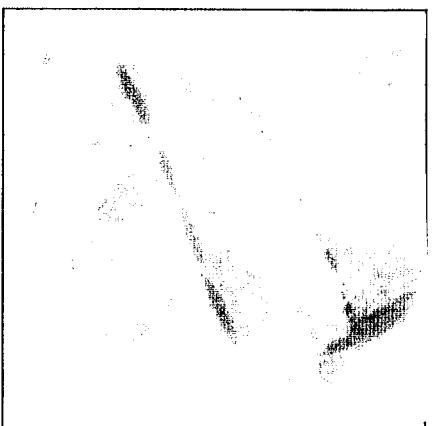


Figure 16 : Intra granular cracking, with birth and growth of macro defects together.

succed to elucidate these structure by T.E.M observations due to the inhomogeneity of the shocked samples.

5. DISCUSSION

It seems to us that the proposal of "damping power" Ω^{-1} is able to control the shock damping of SMA. Many mechanical parameters have to be mastered, particularly the strain rate sensitivity, studied elsewhere [10]. Both methods used, the microstructure is heterogeneous, may be due the strain rate increases then decreases at the end of the shock (in fact, elastic stress waves are followed by plastic waves, then by unloading stress waves, which are probably the most drastic for the microstructure). The higher the shock energy (and the strain rate), the more the temperature variation is. This evidence allows us to singularize alloys with a high shape memory effect : for example Cu-Zn-Al alloy before and after quenching treatment. The consequence of the heterogeneous deformation is detected on the microstructures : on polycrystalline specimens, it was difficult to find an evolution related to the shock energy. We have found new martensites structures as shown by X-ray diffraction and DSC. The transformation temperature would be slightly lowered. Optical micrography shows concentrated martensitic structures at grain boundaries. It is thought of a succession of phase transformations till persistent damages : cracks were observed in that look like adiabatic shear bands and wedge at grain boundaries junctions. The alloy accommodates the heterogeneous deformations such a way it is difficult to precise on polycrystalline samples. Finally after the plastic deformation of austenite, martensites appear and are deformed till crack formation where the plastic instability will be very high.

6. CONCLUSIONS

The elementary definition of "damping power" Ω^{-1} appears a way to analyse the shock resistance of shape memory alloys by both used methods. However the relation $\Omega^{-1}(\dot{\epsilon})$ is not completely mastered. The microstructural evolution depends on the strain rate $\dot{\epsilon}$. It was only shown the appearance of new martensite phases to accommodate the deformation, but the heterogeneous structure shows also damages like cracks, wedges and cavities.

Acknowledgement

We thank M.DANNAWI (Ecole Centrale de Nantes) for his efficient contribution to this study especially for mechanical behaviour understanding.

REFERENCES

- [1] GUENIN.G, Mise au point d'un ensemble de mesures ultra-sonores., Application à l'étude du LiF écroui, Thèse INSA de Lyon (1971)
- [2] DELAEY.L et DERUYTTERE.A (1978) "Shape Memory Effect, Super-elasticity and Damping in Copper-Zinc-Aluminium Alloys", Report 78R1, Katholieke Universiteit Leuven, Belgium
- [3] SUGIMOTO.K, Basic and Applied Research on High Damping Alloys for Application to Noise Control, Mem.Inst.Sci.Ind.Res. Osaka Univ 35 (1978) 31-44
- [4] DE JONGHE.W, DE BATIST.R et DELAEY.L, in "Shape Memory Effect in Alloys" édité par J.PERKINS, Plenum Press (1975) 451 et Metal Science, 11 (1977) 523
- [5] KOSHIMIZU.K, Etude par frottement intérieur d'une transformation martensitique, Thèse EPFL Lausanne (1981)
- [6] DELORME.J.F, SCHMIDT.J, ROBIN.M et GOBIN.P.F, Journal de Physique, Colloque C2, Suppl. au n°7 tome 32 (1971) 101
- [7] MERCIER.O et MELTON.K.N, Acta Met. 27 (1979) 1467
- [8] BELKO.V.N, DARINSKIY.B.M, POSTNIKOV.V.S et SHARSHAKOV.I.M, Physics of Metals and Metallography, 27 (1969) 140
- [9] K.OGAWA, Characteristics of shape memory alloy at high strain rate, Journal de Physique, Colloque C3, Suppl.N°9, Tome 49 (1988) C3-115 à 120
- [10] J.MULLER, Contribution à la connaissance de la capacité d'amortissement des chocs dans les alliages à mémoire de forme, Thesis, Université Paris 6 (1991)